ChemComm

Pnictogen bonding at the service of gold catalysis: The case of a phosphinostiborane gold complex

Journal:	*ChemComm*
Manuscript ID	CC-COM-10-2023-004942.R1
Article Type:	Communication

Pnictogen bonding at the service of gold catalysis: The case of a phosphinostiborane gold complex

Received 00th January 20xx,
Accepted 00th January 20xx

DOI: 10.1039/x0xx00000x

Benyu Zhou,[a] Shantabh Bedajna[a] and François P. Gabbaï*[a]

The search for alternative gold catalyst activators has led us to consider the design of platforms in which a phosphine gold chloride moiety could be activated via formation of a pnictogen bond with a neighboring antimony unit. Here, we describe that such a system can be accessed from 4-(diphenylphosphino)-5-(diphenylstibino)-2,7-di-*tert*-butyl-9,9-dimethylxanthene, by oxidation of the stibine with 3,5-di-*tert*-butyl-*o*-benzoquinone and by coordination of an AuCl unit to the phosphine. This strategy affords a complex in which a Lewis acidic or pnictogen-bond donor catecholatostiborane unit flanks the adjacent gold chloride moiety. This design impacts the catalytic reactivity of the gold center, as reflected by the ability of this complex to catalyze propargyl amide cyclization reactions. Comparisons with a phosphinostiborane ferrocene analog and computations point to the formation of an intramolecular Au-Cl→Sb(V) as responsible for the observed catalytic activity.

The utilization of gold(I) chloride complexes [LAuCl] as precatalysts for alkyne activation is a well-established practice.[1] However, their efficacy relies on a chloride anion abstractor, often in the form of a silver salt (Figure 1). This requirement introduces complications due to the need for an additional reaction step and the light sensitivity and hygroscopic nature of silver salts.[2] Moreover, the irreversibility of chloride abstraction reactions leaves the gold metal exposed, rendering it susceptible to decomposition.[3] Consequently, novel strategies to activate Au-Cl bonds that circumvent these challenges have become coveted. Recent endeavors in this direction have probed the ability of hydrogen bond donor groups to engage and thus activate the Au-Cl bond. This strategy has met significant success with simple additives such as $(CF_3)_2CHOH$[4] or internally installed amide, urea, or squaramide functionalities positioned to engage the Au-Cl bond.[5] Building on the parallels that connect hydrogen bonding to σ hole interactions, approaches that rely on halogen, chalcogen and pnictogen bonding have also surfaced. One of the earliest examples came from Huber who showed that halogen bond donors such as **A** could also be used for this purpose and efficiently activate gold-based carbophilic catalysts (Figure 1).[6] This contribution, which has now been elaborated upon,[7] prompted us to test the use of highly chloridophilic chalcogen bond donors such as **B**, a bifunctional telluronium cation particularly well adapted to the activation Au-Cl and Pt-Cl bonds. Bearing in mind that Lewis acidity culminates in the lower part of the group 15, we have also contemplated approaches based on pnictogen bonding. Our original efforts centered on the intramolecular positioning of a mildly chloridophilic dichlorostibine unit as in the gold complex **C**, which displayed carbophilic reactivity in the absence of any activators.[8] This activity was assigned to the ability of dichlorostibine unit to engage the gold-bound chloride via one of its vacant sites.

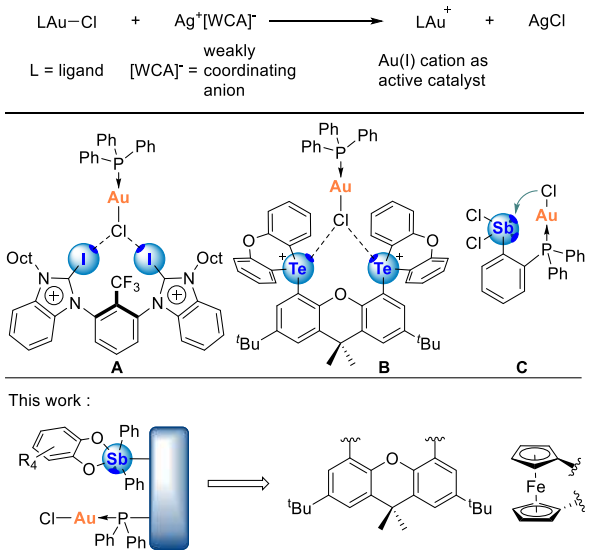

Figure 1. Strategies for the activation of gold chloride complexes and objective of this work

Our research, coupled with the contributions of others, has shown that the oxidation of stibines into stiboranes provides an efficient means for enhancing pnictogen bonding via a deepening of the σ holes and a lowering of the σ*-orbitals energies.[9] This enhancement, which is easily induced through oxidation of the antimony center using an *ortho*-quinone, has led to numerous applications in halide anion capture and sensing. Building on these earlier results and realizing that pnictogen bonding with Sb(V) could also serve for the silver-free

[a] *Department of Chemistry, Texas A&M University, College Station, TX 77843, USA. E-mail: francois@tamu.edu*

† *Electronic supplementary information (ESI) available: Additional experimental and computational details and crystallographic data in cif format. CCDC 2299051-2299054. For ESI and crystallographic data in CIF or other electronic format see XXXXXXXXXXX*

activation of gold chloride catalysts, we are now considering constructs in which an AuCl moiety is positioned in proximity to a stiborane. The findings presented in this paper provide support for this design and reveal that pnictogen bonding in the pentavalent state may be an effective enabler for gold catalysis.

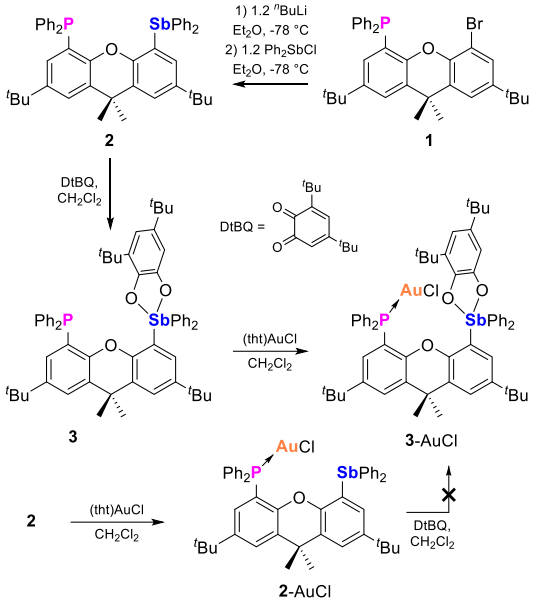

Scheme 1. Synthesis of the phosphine-stibine ligand **2**, along with its auration and oxidation.

To test this idea, we selected two phosphinostibines based either on a 2,7-di-*tert*-butyl-9,9-dimethylxanthene-4,5-diyl or 1,1'-ferrocenediyl backbone (*vide infra*). The first one was synthesized starting from the known 4-diphenylphosphino-5-bromo-2,7-di-*tert*-butyl-9,9-dimethylxanthene (**1**)[10] which was lithiated and subsequently allowed to react with an excess of Ph_2SbCl, yielding the targeted 4-diphenylphosphino-5-diphenylstibino-2,7-di-*tert*-butyl-9,9-dimethylxanthene (**2**) in 69% yield (Scheme 1). Compound **2** has been fully characterized. Its $^{31}P\{^1H\}$ NMR spectrum displays a single resonance at -16.2 ppm, a chemical shift consistent with that of 4,5-bis(diphenylphosphino)-2,7-di-*tert*-butyl-9,9-dimethylxanthene (-16.2 ppm).[11] The solid-state structure of **2,** confirmed by single crystal X-ray diffraction, showed a P-Sb separation of 4.227(7)-4.261(3) Å, which provides a spacious pocket for metal coordination to the phosphine center.

The reactivity of this non-symmetrical ligand was first probed with a focus on the metalation of the phosphine center and oxidation of the antimony (III) center (Scheme 2). Initial oxidation trials targeting the stibine center involved the reaction of **2** with one equivalent of *o*-chloranil. Analysis of the resulting reaction mixture's $^{31}P\{^1H\}$ NMR spectrum indicated a partial oxidation of the phosphine center; however, no pure product was successfully isolated. This non-selective oxidation tendency of *o*-chloranil towards both a phosphine and a stibine moiety has been observed previously,[12] underscoring the excessively oxidizing nature of *o*-chloranil. Interestingly, when the reaction was repeated with a less potent *o*-quinone, namely 3,5-di-*tert*-butyl-*o*-benzoquinone (DtBQ), a complete conversion to a new species, designated as **3**, was observed. Subsequent analysis revealed that this new species is a phosphinestiborane compound as a result of selective oxidation of the stibine center with the quinone. The $^{31}P\{^1H\}$ NMR spectrum of compound **3** showed a singlet at -22.7 ppm, significantly shifting upfield from that of **2** (-16.2 ppm). The molecular structure of **3** was confirmed by single crystal X-ray diffraction (Figure 2), which shows that the stiborane adopts a distorted square pyramidal geometry characterized by the τ_5 value of 0.22. This structure also suggests that the phosphorus and antimony moieties are bent inward as if pulled toward one another. The resulting P-Sb separation of 3.9248(5) Å is slightly longer than the sum of the van der Waals radii of the two atoms (~3.86 Å),[13] suggesting insignificant P→Sb orbital-based bonding. The proximity of the phosphorus atom and stiboranes moiety indicates that the upfield shift of the $^{31}P\{^1H\}$ NMR resonance of **3** may result from the magnetic anisotropy associated to the catecholato ligand, the aromatic ring of which directly faces the phosphorus atom. Treatment of **3** with one equivalent of (tht)AuCl furnishes the desired gold complex **3**-AuCl in a 96% yield. Fortunately, single crystals of compound **3**-AuCl are easily obtained, facilitating the elucidation of its solid-state structure (Figure 2). The stiborane adopts a distorted square pyramidal geometry characterized by a τ_5 value of 0.37. Even if no conspicuously short contacts could be detected, the Au-Cl moiety is oriented toward the open face of the stiboranes

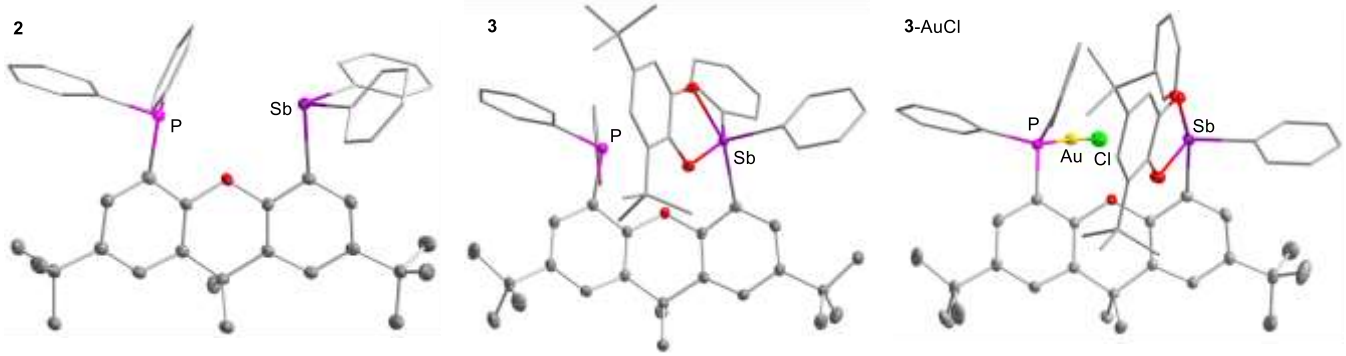

Figure 2. Crystal structures of compounds **2**, **3**, and **3**-AuCl.

moiety. As a side note, we also tested access to **3**-AuCl via an auration-first-oxidation-second approach. Even if **2** could be easily converted into **2**-AuCl, this gold complex, characterized by X-ray diffraction and NMR spectroscopy, failed to react with 3,5-di-*tert*-butyl-*o*-benzoquinone, underscoring importance in which the synthetic steps in Scheme 1 need to be carried out. The inertia of the gold center to oxidation by the *ortho*-quinone is consistent with a recent report which showed that Ph_3PAuCl does not react with DtBQ.[14]

Even if no short contacts are observed between the gold chloride and the stiborane unit, we became interested in determining the electrostatic characteristics of the open, Lewis acidic face of the stiborane. Toward this end, we truncated the phosphine gold chloride unit of **3**-AuCl to generate the model dimethylxanthyl-stiborane **D** (Figure 3). Visualisation of the molecular electrostatic potential (ESP) of this model derivative allows for the identification of a σ hole associated to a $V_{s,max}$ of 28.0 kcal/mol when the ESP map is drawn with an isovalue of 0.0015 atomic units (a.u.).[15] The surface point associated with this elevated potential stands at 2.056 Å from the antimony atom, a value very close to the van der Waals radius of this element (2.06 Å),[13] thus indicating its pertinence with regards to assessing the engagement of the antimony center in weak σ hole interactions such as with the nearby the gold chloride moiety.

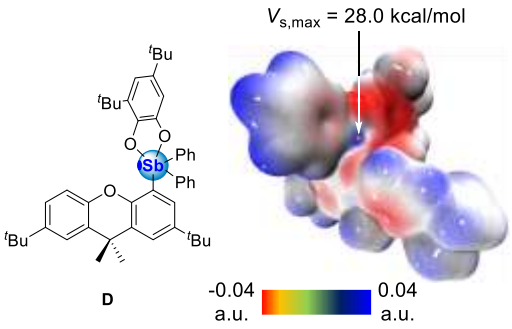

Figure 3. Optimized structure and electrostatic potential maps of **D**.

Equipped with this knowledge, we became eager to test the ability of **3**-AuCl to act as a carbophilic catalyst that would self-activate through engagement of the gold-bound chloride by the stiborane. For comparative purposes, we also included the analogous ferrocene-based system **5**-AuCl which could be easily generated from the recently reported complex **4**-AuCl[12] with 3,5-di-*tert*-butyl-*o*-benzoquinone (Scheme 2). This complex, characterized by a $^{31}P\{^1H\}$ NMR resonance at 28.0 ppm, was isolated as a yellow, diamagnetic air stable solid and used as a carbophilic catalyst. We speculated that this system would provide for a lower level of preorganization, given low rotation barrier reported for ferrocene.[16] We tested these complexes as catalysts for the cycloisomerization of the propargyl amide substrate **6** which did not proceed, even upon heating to 50 °C in $CDCl_3$. By contrast, we observed the onset of a reaction and formation of the corresponding methyleneoxazole **7** when **3**-AuCl (2 mol%) was employed as a catalyst under the same conditions. Monitoring of this reaction for 2 hours, afforded the data plotted in Figure 4, illustrating the progress of the reaction. After a brief induction period, **3**-AuCl proved to be the best catalyst. These initial results support the notion that the Sb(V) center of **3**-AuCl engages the Au-Cl bond, rendering the gold center more carbophilic and consequently more active toward

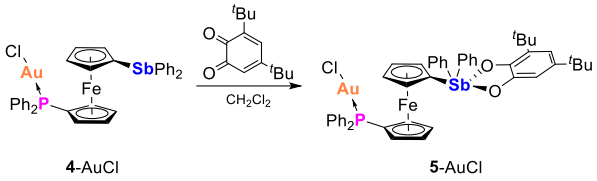

4-AuCl **5**-AuCl

Scheme 2. Synthesis of the ferrocene-based complex **5**-AuCl.

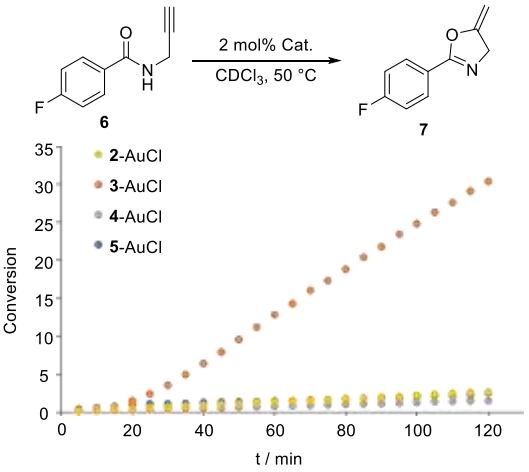

Figure 4. Cycloisomerization of propargyl amide **6** as a function of time in the presence of different catalysts. See figure for conditions.

the propargyl amide. To assess the impact of antimony oxidation, we also tested the corresponding Sb(III) complex **2**-AuCl and observed <3% conversion at the same time point under identical conditions, underscoring the Lewis acidity at the antimony center as a critical factor. The ferrocene-based catalyst **5**-AuCl showed only a modicum of activity. Presumably, the ability of the ferrocene unit to rotate leads to a less ideally preorganized arrangement of the gold chloride and stiborane units, impeding activation of the Au-Cl bond by the pentavalent antimony center. Finally, we also tested **2**-AuCl (2 mol%) as a

catalyst in the presence of an equimolar amount of AgOTf, which led to a conversion of 18% after 2h vs. 30% when **3**-AuCl was employed. This last comparison highlights the benefits of our approach and shows that an intramolecularly installed stiborane provides a superior activation than an added silver salt.

To provide a model that would allow to explain the above catalytic results, we computed the structure of the putativte adduct formed between **3**-AuCl and the substrate (Figure 5). The optimized structure of the this adduct shows coordination of the alkyne to the gold center with concomitant shifting of the chloride ligand towards the Lewis acidic antimony center. The newly formed Au-Cl→Sb interaction leaves the gold center more exposed and thus better predisposed to electrophilically activate the substrate. We will note in passing that catecholatostiboranes have a demonstrated ability to complex halide anions, including chloride, to form the corresponding haloantimonate.[9a, 9c] These precedents support the viability of the Au-Cl→Sb interaction identified computationally.

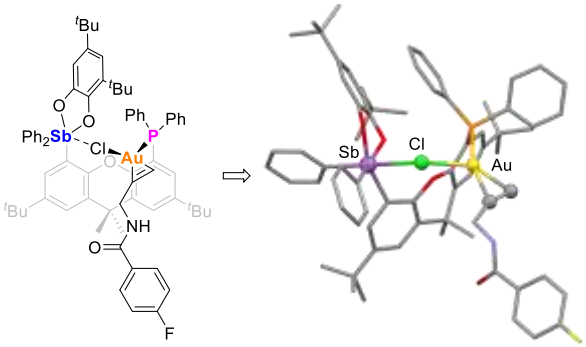

Figure 5. Computationally modeled gold-alkyne complex showing a possible activation mode. This adduct is 25.7 kcal/mol above **3**-AuCl and **6**.

In summary, we describe a new strategy for the construction of a self-activating gold catalyst. The self-activating properties of this catalyst derive from incorporating a catecholatostiborane unit positioned next to the gold chloride moiety. We propose that the convergence of these two functionalities sets the stage for an intramolecular Au-Cl→Sb(V) interaction, the formation of which benefits from the unique pnictogen bond donor or Lewis acidic properties of the antimony compound. Catalysis experiments involving propargyl amides and their cycloisomerization support this proposal and also show that oxidation of the antimony center from the +III to the +V oxidation state turns on the carbophilic reactivity of the gold center.[17]

Acknowledgements

This work was supported by the U.S. Department of Energy, Office of Science, Basic Energy Sciences (DE-SC0023269) and the Welch Foundation (A-1423). All calculations were conducted with the advanced computing resources provided by the Texas A&M High-Performance Research Computing facility.

References

1. a) A. S. K. Hashmi, *Chem. Rev.*, 2007, **107**, 3180-3211; b) N. Marion and S. P. Nolan, *Chem. Soc. Rev.*, 2008, **37**, 1776-1782; c) A. Arcadi, *Chem. Rev.*, 2008, **108**, 3266-3325; d) D. J. Gorin, B. D. Sherry and F. D. Toste, *Chem. Rev.*, 2008, **108**, 3351-3378; e) E. Jimenez-Nunez and A. M. Echavarren, *Chem. Rev.*, 2008, **108**, 3326-3350.
2. a) D. Weber and M. R. Gagné, *Org. Lett.*, 2009, **11**, 4962-4965; b) D. Wang, R. Cai, S. Sharma, J. Jirak, S. K. Thummanapelli, N. G. Akhmedov, H. Zhang, X. Liu, J. L. Petersen and X. Shi, *J. Am. Chem. Soc.*, 2012, **134**, 9012-9019; c) A. Homs, I. Escofet and A. M. Echavarren, *Org. Lett.*, 2013, **15**, 5782-5785; d) A. Zhdanko and M. E. Maier, *ACS Catal.*, 2015, **5**, 5994-6004.
3. W. Wang, G. B. Hammond and B. Xu, *J. Am. Chem. Soc.*, 2012, **134**, 5697-5705.
4. a) M. Kato, Y. Ueta and S. Ito, *Chem. Eur. J.*, 2021, **27**, 2469-2475; b) N. V. Tzouras, A. Gobbo, N. B. Pozsoni, S. G. Chalkidis, S. Bhandary, K. Van Hecke, G. C. Vougioukalakis and S. P. Nolan, *Chem. Commun.*, 2022, **58**, 8516-8519; c) P. Elías-Rodríguez, E. Matador, M. Benítez, T. Tejero, E. Díez, R. Fernández, P. Merino, D. Monge and J. M. Lassaletta, *J. Org. Chem.*, 2023, **88**, 2487-2492.
5. a) Z. Zhang, V. Smal, P. Retailleau, A. Voituriez, G. Frison, A. Marinetti and X. Guinchard, *J. Am. Chem. Soc.*, 2020, **142**, 3797-3805; b) O. Seppänen, S. Aikonen, M. Muuronen, C. Alamillo-Ferrer, J. Burés and J. Helaja, *Chem. Commun.*, 2020, **56**, 14697-14700; c) A. Franchino, À. Martí, S. Nejrotti and A. M. Echavarren, *Chem. Eur. J.*, 2021, **27**, 11989-11996.
6. J. Wolf, F. Huber, N. Erochok, F. Heinen, V. Guérin, C. Y. Legault, S. F. Kirsch and S. M. Huber, *Angew. Chem. Int. Ed.*, 2020, **59**, 16496-16500.
7. A. Boelke, T. J. Kuczmera, E. Lork and B. J. Nachtsheim, *Chem. Eur. J.*, 2021, **27**, 13128-13134.
8. a) J. S. Jones and F. P. Gabbaï, *Chem. Eur. J.*, 2017, **23**, 1136-1144; b) L. C. Wilkins, Y. Kim, E. D. Litle and F. P. Gabbaï, *Angew. Chem. Int. Ed.*, 2019, **58**, 18266-18270; c) W.-C. Liu and F. P. Gabbaï, *Chem. Sci.*, 2023, **14**, 277-283; d) B. Zhou and F. P. Gabbaï, *J. Am. Chem. Soc.*, 2021, **143**, 8625-8630.
9. a) R. R. Holmes, R. O. Day, V. Chandrasekhar and J. M. Holmes, *Inorg. Chem.*, 1987, **26**, 157-163; b) M. Yang, D. Tofan, C.-H. Chen, K. M. Jack and F. P. Gabbaï, *Angew. Chem. Int. Ed.*, 2018, **57**, 13868-13872; c) B. L. Murphy and F. P. Gabbaï, *J. Am. Chem. Soc.*, 2023, **145**, 19458–19477.
10. E. Zuidema, P. E. Goudriaan, B. H. G. Swennenhuis, P. C. J. Kamer, P. W. N. M. van Leeuwen, M. Lutz and A. L. Spek, *Organometallics*, 2010, **29**, 1210-1221.
11. L. A. van der Veen, P. C. J. Kamer and P. W. N. M. van Leeuwen, *Organometallics*, 1999, **18**, 4765-4777.
12. J. Schulz, J. Antala, D. Rezazgui, I. Císařová and P. Štěpnička, *Inorg. Chem.*, 2023, **62**, 14028–14043.
13. M. Mantina, A. C. Chamberlin, R. Valero, C. J. Cramer and D. G. Truhlar, *J. Phys. Chem. A*, 2009, **113**, 5806-5812.
14. G. Szalóki, J. Babinot, V. Martin-Diaconescu, S. Mallet-Ladeira, Y. García-Rodeja, K. Miqueu and D. Bourissou, *Chem. Sci.*, 2022, **13**, 10499-10505.
15. T. Lu and F. Chen, *J. Comput. Chem.*, 2012, **33**, 580-592.
16. a) M. T. Islam, S. P. Best, J. D. Bourke, L. J. Tantau, C. Q. Tran, F. Wang and C. T. Chantler, *J. Phys. Chem. C*, 2016, **120**, 9399-9418; b) D. Astruc, *Eur. J. Inorg. Chem.*, 2017, **2017**, 6-29.
17. H. Yang and F. P. Gabbaï, *J. Am. Chem. Soc.*, 2015, **137**, 13425-13432.